Direct Imaging of Lipid-Ion Network Formation under Physiological Conditions by Frequency Modulation Atomic Force Microscopy

Takeshi Fukuma, Michael J. Higgins, and Suzanne P. Jarvis

Centre for Research on Adaptive Nanostructures and Nanodevices, Lincoln Place Gate, Trinity College Dublin, Dublin 2, Ireland

(Received 11 December 2006; published 5 March 2007)

Various metal cations in physiological solutions interact with lipid headgroups in biological membranes, having an impact on their structure and stability, yet little is known about the molecular-scale dynamics of the lipid-ion interactions. Here we directly investigate the extensive lipid-ion interaction networks and their transient formation between headgroups in a dipalmitoylphosphatidylcholine bilayer under physiological conditions. The spatial distribution of ion occupancy is imaged in real space by frequency modulation atomic force microscopy with sub-Ångstrom resolution.

DOI: 10.1103/PhysRevLett.98.106101 PACS numbers: 68.37.Ps, 68.55.−a, 81.07.−b, 87.14.Cc

Under physiological conditions, biological membranes are surrounded by an electrolytic solution containing various metal cations. The influence of these cations on membrane structure and stability has been studied intensively using model lipid bilayers. The addition of salts can trigger lipid bilayer phase separation [1–3] and vesicle aggregation and fusion processes [4,5]. The striking influence of the ions has highlighted the importance of lipid-ion interactions in biological processes.

So far, a number of spectroscopy experiments have revealed that metal cations specifically interact with negatively charged moieties of the lipid headgroups [6–9]. These experiments, together with theoretical simulations [10], have led to the idea that individual ions may be interacting with multiple headgroups to form complex ''lipid-ion networks.'' This idea has been used to account for the observed influence of the ions such as enhanced mechanical strength of membranes [11] and reduced mobility of the lipid molecules therein [12].

However, it has been a great challenge to experimentally access such lipid-ion networks due to the lack of a method able to investigate local lipid-ion interactions with Ångstrom resolution. Here we investigate the lipid-ion networks and their transient formation between lipid headgroups with sub-Ångstrom resolution by frequency modulation atomic force microscopy (FM-AFM) [13].

FM-AFM has been used mainly for atomic-scale imaging in ultrahigh vacuum [14,15], and its application in liquid has been very limited [16]. Recently, it has become possible to obtain true atomic resolution with piconewton order loading forces even in liquid [17] using an ultralow noise cantilever deflection detection system [18], enabling extremely small amplitude cantilever oscillations [19].

We have investigated a mica supported dipalmitoylphosphatidylcholine (DPPC) lipid bilayer in a phosphate buffer saline (PBS) solution as a model biological membrane under physiological conditions. A DPPC molecule has a zwitterionic phosphatidylcholine (PC) headgroup consisting of a negatively charged phosphate and a positively charged choline group [Fig. 1(a)]. DPPC molecules spontaneously form a bilayer in aqueous solution with the hydrophilic headgroups in contact with water and hydrophobic alkyl chains inside the bilayer.

The PBS solution used in this experiment contains 153.2 mM Na^+, 4.17 mM K^+, 139.7 mM Cl^-, and 9.57 mM PO_4^{3-}. This ion content is a good mimic for the physiological environment of the extracellular membrane surface of mammalian cells [20]. The DPPC bilayer on mica was formed by the vesicle fusion method [21]. All of the experiments were performed in PBS solution at room temperature (21 °C), where the DPPC bilayer is in gel phase with relatively low fluidity.

A homebuilt FM-AFM [22] was used in this experiment. The tip-sample distance regulation was operated in the constant frequency shift (Δf) mode. A silicon cantilever (NCH: Nanosensors) with a spring constant of 34 N/m, and a resonance frequency of 134 kHz determined in the PBS solution, was used. The cantilever was oscillated at a constant amplitude of 0.29 nm. The Δf values during the FM-AFM imaging were kept within the range of ±20 Hz (including fluctuations caused by noise), which corresponds to a loading force of ±20 pN as determined from a calculated force curve [23]. When the spatial resolution is

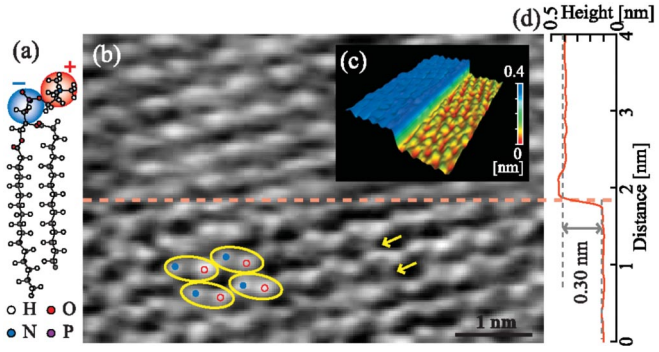

FIG. 1 (color). (a) Structure of DPPC. (b) Line-by-line flattened FM-AFM image of a DPPC bilayer in PBS solution. Tip velocity: 146 nm/s. (c) 3D view of (b). (d) Line-averaged height profile of (b).

defined as the separation between the closest two peaks resolved in an image, the highest lateral resolution obtained in this experiment was 90 pm.

The force vs distance curves measured with an AFM tip on a flat surface in aqueous solution often show oscillatory profiles corresponding to the sequential removal of structured water molecules between the tip and the sample as observed previously for this system [24]. In order to image the lipid surface, the tip must interact directly with the lipids, not with an intermediary hydration shell. We found that the FM-AFM images obtained at the water-lipid interface often show spontaneous jumps as shown in Fig. 1. The observed height changes are in the range of 0.2–0.3 nm [Fig. 1(d)], which agrees well with the size of a water molecule. This suggests that the observed height changes are due to the hydration shell between the tip and the sample [25]. Note that such spontaneous jumps can take place more than once in one image without changing scan conditions.

The upper half of Fig. 1(b) shows molecular-scale corrugations corresponding to lipid headgroups imaged with an intermediary hydration shell. The lower half of Fig. 1(b) shows pairs of two protrusions separated by about 0.30 nm as indicated by yellow circles. From the separation and the structure of the lipid, we attribute these two protrusions to choline and phosphate groups in the PC headgroup. Although we cannot differentiate choline and phosphate groups only from the image, the headgroups are likely to be oriented in the same direction as indicated by the dots in Fig. 1(b). This is because this arrangement is energetically beneficial due to the charge pairing between the alternately positioned negatively and positively charged subgroups [26]. This is also consistent with a previous study by molecular mechanics calculation, where a similar arrangement is proposed as the most favorable arrangement of the PC headgroups [27].

We found that the membrane surface presents various structures depending on both time and location, reflecting the mobile nature of the ions interacting with the lipids. FM-AFM images reveal the existence of at least two clearly different configurations as shown in Figs. 2(a) and 2(b), which are referred to as structures 1 and 2, respectively. Structure 1 is the same as the one shown in the lower half of Fig. 1(b) and shows PC headgroups not associated with ions or water molecules except for the possible bridging below the headgroups [e.g., arrows in Fig. 1(b)]. Structure 2 is characterized by hexagonally arranged surface groups consisting of two oval-shaped subunits with their longer axes parallel to each other. Most of the subunits are oriented in similar directions, indicating that the lipid ordering in the gel phase may put some constraints on the headgroup orientation. Note that the orientation of the subunits is not perfectly uniform or exactly parallel to the fast scan direction, and, hence, the observed features cannot be scan-related artifacts.

The subunits in structure 2 cannot be attributed to the phosphate and choline groups because of the short distance

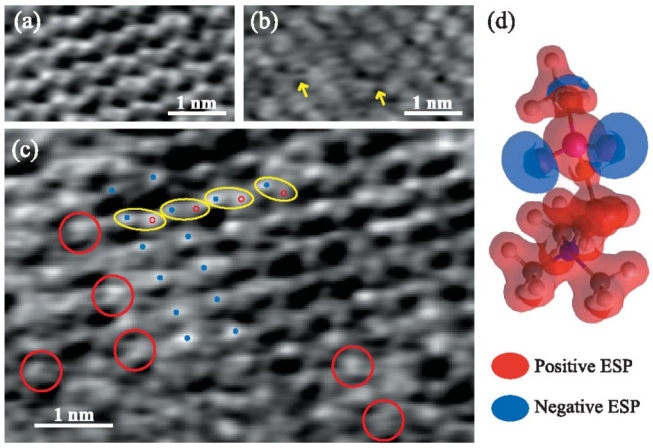

FIG. 2 (color). FM-AFM images of the DPPC bilayer in PBS solution. Height scale: 0.12 nm. (a) Structure 1. Tip velocity: 146 nm/s. (b) Structure 2. Tip velocity: 120 nm/s. (c) Transient region between structures 1 and 2. Tip velocity: 146 nm/s. (d) ESP distribution of a methyl-terminated PC headgroup simulated by MOPAC [29].

between the two (0.1–0.2 nm). The distance between the apposing subunits is even smaller than the diameter of a single atom. In order to obtain such subatomic-scale contrast in FM-AFM, the tip-sample interaction force must be dominated by the short-range electrical interaction between the tip front atom (or surface atom) and charge distribution of the surface (or tip front atom) [19,28]. For example, Hembacher *et al.* utilized a small atom (carbon atom of the graphite surface) as a probe to image the charge distribution of a tungsten atom at the end of the tip [28]. In contrast to their experiments, the subatomic-scale contrasts in Fig. 2(b) show variations even within the same scan line, so in this case they must represent charge distribution of the surface rather than that of the tip front atom.

The ions are expected to be moving much faster than the time scale of the AFM image acquisition (>10 sec). Since the ions are charged entities, their spatial distribution is directly related to the surface charge distribution. Therefore, the subatomic-scale contrasts observed in Fig. 2(b) are likely to represent averaged positions of mobile ions or, in other words, spatial distribution of ion occupancy. The subunits observed in Fig. 2(b) show various shapes with vague outlines, indicating the mobile nature of the ions associated with the headgroups. The image also shows faint "wirelike" contrast between adjacent subunits as indicated by the arrows. This implies that ions are moving back and forth between adjacent subunits to create charge distribution between them. The neighboring headgroups are sharing such ion charge, through which they interact with each other. Figure 2(b) clearly visualizes lateral organization of such interheadgroup interaction mediated through the ions, namely, lipid-ion networks. This interpretation is consistent with our previous experiments carried out in pure water [24], where, although we have been able to image individual lipid headgroups of the DPPC

bilayer, we have never observed structure 2 in the absence of ions.

The tip used in this experiment is made of silicon, so the tip apex is covered with a native silicon oxide layer. There are two possible atom species that could be the tip front atom under these experimental conditions: oxygen or hydrogen. It is very unlikely for a silicon atom to be the front atom. Dangling bonds of a silicon atom are so reactive that they must be terminated with hydrogen or oxygen atoms in air or liquid. These tetrahedrally coordinated atoms make it impossible for a silicon atom to directly interact with surface charges. Although we cannot determine whether the front atom is oxygen or hydrogen, these atoms are comparable to or even smaller than the carbon atom used in Ref. [28], which may account for the high spatial resolution obtained in this experiment.

Figure 2(c) shows an FM-AFM image of a transient region between structures 1 and 2, showing various intermediate configurations. From the center to the right, the image shows pairs of protrusions that are characteristic of structure 1 as indicated by the ovals. Assuming the periodicity of these two protrusions as indicated by the dots, we found that most of the bright spots are located at the positions of the solid blue dots. Furthermore, some of the bright spots indicated by the circles show oval-shaped subunits that are characteristic of structure 2. They are also located at the positions corresponding to the solid dots. This result strongly suggests that the surface groups in structure 2 are either phosphate or choline groups associated with ions.

Each of the surface groups consists of two subunits, suggesting the existence of two ion-binding sites for each surface group. The phosphate group has two negatively charged oxygen atoms accessible to cations such as Na^+ and K^+, while the positively charged nitrogen atom in the choline group is surrounded by four methyl groups and is, hence, hardly accessible to anions such as Cl^- and PO_4^{3-}. The electrostatic potential (ESP) distribution of the PC headgroup simulated by MOPAC [29] [Fig. 2(d)] reveals the two localized negative ESP distributions around the two equivalent oxygens, showing remarkable resemblance to the two subunits imaged in Fig. 2(b). Therefore, the surface group is more likely to be a phosphate group associated with cations than a choline group associated with anions. This is consistent with previous studies by IR spectroscopy [9] and molecular dynamics simulations [12,30]. These studies have suggested that the metal cations specifically bind to phosphate groups, while chloride anions remain solvated near the surface.

Although we cannot differentiate Na^+ and K^+ from the images alone, there are two reasons to suggest that the lipid-ion networks are likely to be predominantly formed by Na^+. First, the concentration of Na^+ (153.2 mM) is more than 30 times higher than that of K^+ (4.17 mM) in the PBS solution used in this experiment. Thus, Na^+ must predominate even if they have the same affinity to the binding site. Second, scanning differential calorimetry [31] and IR spectroscopy [9] experiments consistently suggested that the order of association between monovalent cations and phosphate groups follows $Li^+ > Na^+ > K^+$. Thus, Na^+ is expected to more strongly interact with phosphate groups than K^+.

Because of the energy costs associated with the dehydration of solvated ions and of ions approaching against the positive surface potential created by the other cations bound to the surface, the density of Na^+ ions associated with zwitterionic but neutral PC headgroups is expected to be very small. In fact, electrophoretic mobility measurements [32] and molecular dynamics simulations [30] have suggested that the binding coefficient of Na^+ ions to PC headgroups is 0.15–0.6 M^{-1} (2–9 ions per 100 lipids for a 150 mM NaCl solution). However, it is also known that even such a small number of Na^+ ions can significantly increase the mechanical strength of the bilayers with PC headgroups [11]. To reconcile these two results, Na^+ ions associated with the membrane surface must be laterally moving to interact with a number of different headgroups. This is consistent with our interpretation that the FM-AFM image contrast represents the averaged position of mobile ions.

If the ion binding does not affect the lipid bilayer structure, the ions must be evenly distributed over the surface due to the electrostatic interactions. However, the observation of structure 1 contradicts this and, instead, suggests that the ion binding should cause the bilayer to take an energetically more favorable structure. In fact, averaged lipid spacing in structure 2 (approximately 0.49 nm) is slightly smaller than that in structure 1 (approximately 0.52 nm). Such an increase of packing density may account for the energetic benefit of forming the local lipid-ion complexes. Note that the structure at the membrane surface keeps changing between structures 1 and 2 even at one location. Thus, the electrostatic potential averaged over a long time period (e.g., >10 min) may be uniform across the surface. We observed structure 2 more often than structure 1. This indicates that structure 2 might cover a larger area than structure 1. However, the relative occurrence of structures 1 and 2 may depend on ion concentration; thus, systematic measurements with different ion concentrations would be required to fully quantify the effect of ion binding on a bilayer structure.

High reproducibility of the FM-AFM imaging allows us to take two sequential images of the same area as shown in Figs. 3(a) and 3(b). While some of the surface groups maintain the arrangements of their subunits as indicated by the circles, other surface groups and lipid-ion networks show a significant difference between the two images. In the images, we have indicated some of the networks and subunits by the arrows marked with "N" and "S," respectively. In the first image [Fig. 3(a)], subunit 1 interacts with subunit 2 through network 1. In the next image [Fig. 3(b)], network 1 disappears, and, instead, networks 2–4 are formed. The fact that the network formation and disap-

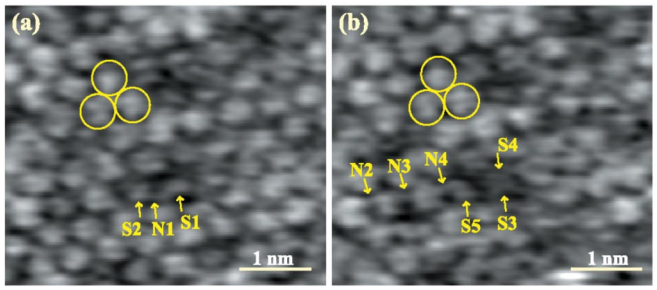

FIG. 3 (color online). Sequential FM-AFM images of the same area of the DPPC bilayer in PBS solution. Height range: 0.1 nm. Tip velocity: 120 nm/s. Imaging speed: 85 s/image.

pearance can be imaged by AFM demonstrates that they are relatively slow processes; namely, spatial distribution of ion occupancy changes in the order of seconds in contrast to the rapid motion of individual ions.

We found that some surface groups change their configurations upon formation or disappearance of lipid-ion networks. For example, subunit 1 is not pairing with another subunit in Fig. 3(a), while a pair of subunits 3 and 4 appears in the next image [Fig. 3(b)] but with a darker contrast than other subunits, suggesting the lower height of this headgroup. It is likely that this particular headgroup was temporarily at an irregular tilt angle due to the interaction between subunits 1 and 2 against the slight height difference when the first image was taken.

The observed structural changes due to the formation and disappearance of the lipid-ion networks are consistent with our interpretation that the negatively charged phosphate groups are sharing the positive charge of cations, by which an attractive electrostatic force is exerted on all of the headgroups involved in the network. The attractive interaction force mediated through such complex lipid-ion networks should bind the headgroups together and increase the global mechanical strength of the membrane. In fact, we have measured the force required to penetrate the DPPC bilayer with an AFM tip by taking static-mode AFM force curves on the bilayers and have obtained 7.0 ± 3.9 nN in water and 36.3 ± 6.2 nN in the PBS solution. The FM-AFM images shown here reveal the submolecular-scale origin of such an influence of ions on the mechanical properties of the membrane.

Under physiological conditions, most of the chemical interactions that determine the structure and functions of biological molecules are mediated through water and ions. FM-AFM provides a powerful means to directly investigate not only the submolecular-scale structure of biological systems but also the spatial distribution and dynamics of the interactions between biological molecules and their physiological environments.

This research was funded by Science Foundation Ireland (Grant No. 01/PI.2/C033) and the Human Frontier Science Program.

[1] M. Rappolt, G. Pabst, H. Amenitsch, and P. Laggner, Colloids Surf. A **183–185**, 171 (2001).
[2] M. Ross, C. Steinen, H.-J. Galla, and A. Janshoff, Langmuir **17**, 2437 (2001).
[3] J. T. Groves, S. G. Boxer, and H. M. McConnell, J. Phys. Chem. B **104**, 11 409 (2000).
[4] S. Ohki, N. Düzgüneş, and K. Leonards, Biochemistry **21**, 2127 (1982).
[5] S. Ohki and K. Arnold, Colloids Surf. B **18**, 83 (2000).
[6] L. Herbette, C. A. Napolitano, and R. V. McDaniel, Biophys. J. **46**, 677 (1984).
[7] C. Altenbach and J. Seelig, Biochemistry **23**, 3913 (1984).
[8] T. R. Hermann, A. R. Jayaweera, and A. E. Shamoo, Biochemistry **25**, 5834 (1986).
[9] H. Binder and O. Zschörnig, Chem. Phys. Lipids **115**, 39 (2002).
[10] M. L. Berkowitz, D. L. Bostick, and S. Pandit, Chem. Rev. **106**, 1527 (2006).
[11] S. Garcia-Manyes, G. Oncins, and F. Sanz, Biophys. J. **89**, 1812 (2005).
[12] R. A. Böckmann, A. Hac, T. Heimburg, and H. Grubmüller, Biophys. J. **85**, 1647 (2003).
[13] T. R. Albrecht, P. Grütter, D. Horne, and D. Ruger, J. Appl. Phys. **69**, 668 (1991).
[14] F. J. Giessibl, Science **267**, 68 (1995).
[15] S. Kitamura and M. Iwatsuki, Jpn. J. Appl. Phys. 2, Lett. **34**, L145 (1995).
[16] S. P. Jarvis, T. Uchihashi, T. Ishida, H. Tokumoto, and Y. Nakayama, J. Phys. Chem. B **104**, 6091 (2000).
[17] T. Fukuma, K. Kobayashi, K. Matsushige, and H. Yamada, Appl. Phys. Lett. **87**, 034101 (2005).
[18] T. Fukuma, M. Kimura, K. Kobayashi, K. Matsushige, and H. Yamada, Rev. Sci. Instrum. **76**, 053704 (2005).
[19] F. J. Giessibl, S. Hembacher, H. Bielefeldt, and J. Mannhart, Science **289**, 422 (2000).
[20] *Molecular Cell Biology*, edited by H. Lodish, A. Berk, S. L. Zipursky, P. Matsudaira, D. Baltimore, and J. Darnell (Freeman, San Francisco, 1999), 4th ed.
[21] *Atomic Force Microscopy in Cell Biology*, edited by B. P. Jena and J. K. H. Hörber (Academic, New York, 2002).
[22] T. Fukuma and S. P. Jarvis, Rev. Sci. Instrum. **77**, 043701 (2006).
[23] J. E. Sader and S. P. Jarvis, Appl. Phys. Lett. **84**, 1801 (2004).
[24] M. Higgins, M. Polcik, T. Fukuma, J. Sader, Y. Nakayama, and S. P. Jarvis, Biophys. J. **91**, 2532 (2006).
[25] T. Fukuma, M. J. Higgins, and S. P. Jarvis, Biophys. J. (to be published).
[26] M. Pasenkiewicz-Gierula, Y. Takaoka, H. Miyagawa, K. Kitamura, and A. Kusumi, Biophys. J. **76**, 1228 (1999).
[27] Y. Nakata, A. Takahashi, and T. Takizawa, J. Chem. Softw. **1**, 39 (1992).
[28] S. Hembacher, F. J. Giessibl, and J. Mannhart, Science **305**, 380 (2004).
[29] J. J. P. Stewart, J. Comput.-Aided Mol. Des. **4**, 1 (1990).
[30] S. A. Pandit, D. Bostick, and M. L. Berkowitz, Biophys. J. **84**, 3743 (2003).
[31] D. Chapmann, W. E. Peel, B. Kingston, and T. H. Lilley, Biochim. Biophys. Acta **464**, 260 (1997).
[32] S. A. Tatulian, Eur. J. Biochemistry **170**, 413 (1987).